

Small-Molecule Procaspase-3 Activation Sensitizes Cancer to Treatment with Diverse Chemotherapeutics

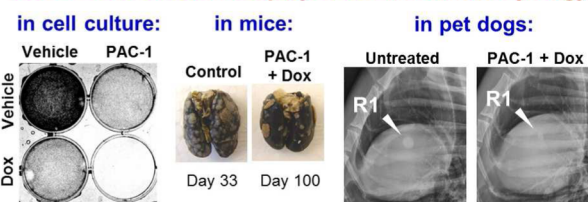
Rachel C. Botham,^{†,‡} Howard S. Roth,[†] Alison P. Book,[§] Patrick J. Roady,^{||} Timothy M. Fan,^{§,‡} and Paul J. Hergenrother^{*,†,‡}

[†]Department of Chemistry, [‡]Institute for Genomic Biology, [§]Department of Veterinary Clinical Medicine, and ^{||}Veterinary Diagnostic Laboratory, University of Illinois Urbana–Champaign, Urbana, Illinois 61801, United States

Supporting Information

ABSTRACT: Conventional chemotherapeutics remain essential treatments for most cancers, but their combination with other anticancer drugs (including targeted therapeutics) is often complicated by unpredictable synergies and multiplicative toxicities. As cytotoxic anticancer chemotherapeutics generally function through induction of apoptosis, we hypothesized that a molecularly targeted small molecule capable of facilitating a central and defining step in the apoptotic cascade, the activation of procaspase-3 to caspase-3, would broadly and predictably enhance activity of cytotoxic drugs. Here we show that procaspase-activating compound 1 (PAC-1) enhances cancer cell death induced by 15 different FDA-approved chemotherapeutics, across many cancer types and chemotherapeutic targets. In particular, the promising combination of PAC-1 and doxorubicin induces a synergistic reduction in tumor burden and enhances survival in murine tumor models of osteosarcoma and lymphoma. This PAC-1/doxorubicin combination was evaluated in 10 pet dogs with naturally occurring metastatic osteosarcoma or lymphoma, eliciting a biologic response in 3 of 6 osteosarcoma patients and 4 of 4 lymphoma patients. Importantly, in both mice and dogs, coadministration of PAC-1 with doxorubicin resulted in no additional toxicity. On the basis of the mode of action of PAC-1 and the high expression of procaspase-3 in many cancers, these results suggest the combination of PAC-1 with cytotoxic anticancer drugs as a potent and general strategy to enhance therapeutic response.

PAC-1 + Doxorubicin display broad anticancer synergy



INTRODUCTION

Cytotoxic chemotherapy formed the foundation of historical cancer treatments, and despite concerted efforts to understand and exploit molecular mechanisms driving cancer growth, cytotoxic chemotherapies remain essential to numerous frontline and salvage treatment protocols.^{1–3} Patients are treated with cytotoxic chemotherapies when targeted agents have not been developed for their malignancy, when they do not respond to targeted therapies, or upon the development of resistance.⁴ Despite the interest in personalized medicine for oncology, the majority of these molecularly targeted therapeutics are not curative when used as single agents.^{5,6} Combination chemotherapy remains the basis for clinical management of diverse cancers, as use of drugs in combinations can increase initial activity or delay the onset of resistance, and tumor cell populations with a high degree of heterogeneity may be eliminated more effectively.^{1,7} Although molecularly targeted agents have been successfully integrated into combination chemotherapy regimens,^{8–10} the inability to reliably predict synergistic activity leads to numerous unsuccessful clinical trials.^{11,12} Furthermore, additive toxicity remains a major limitation; even when drugs are combined as a part of a treatment regimen, they are often administered on schedules that space dosing by a week or more, diminishing the opportunities for true synergistic activity. For example,

doxorubicin is the backbone of many combination therapies, including the MAP protocol (Methotrexate, Adriamycin—brand name of doxorubicin, Cisplatin), used for the treatment of pediatric osteosarcoma¹³ and R-CHOP (Rituximab, Cyclophosphamide, Hydroxydaunorubicin—also known as doxorubicin, Oncovin—also known as vincristine, and Prednisone) for lymphoma.⁹ MAP and R-CHOP are representative of many combination chemotherapy protocols, which were developed to maximize the frequency and intensity of treatment with single agents known to possess activity against the cancer, while avoiding unacceptable levels of toxicity. This is in stark contrast to true cocktail drug therapies, such as those used to treat tuberculosis, where patients are treated daily with up to five different antibiotics, with the goal of eradicating infection and suppressing the development of resistance within a patient.¹⁴ These cocktails are enabled by the high tolerability of the antibiotics, allowing frequent and concurrent treatments. As such, a molecularly targeted therapeutic that broadly synergizes with traditional cytotoxic chemotherapeutics and could be coadministered without additional toxicity would have potential for enormous clinical impact in cancer treatment.

Received: June 7, 2016

Published: July 25, 2016

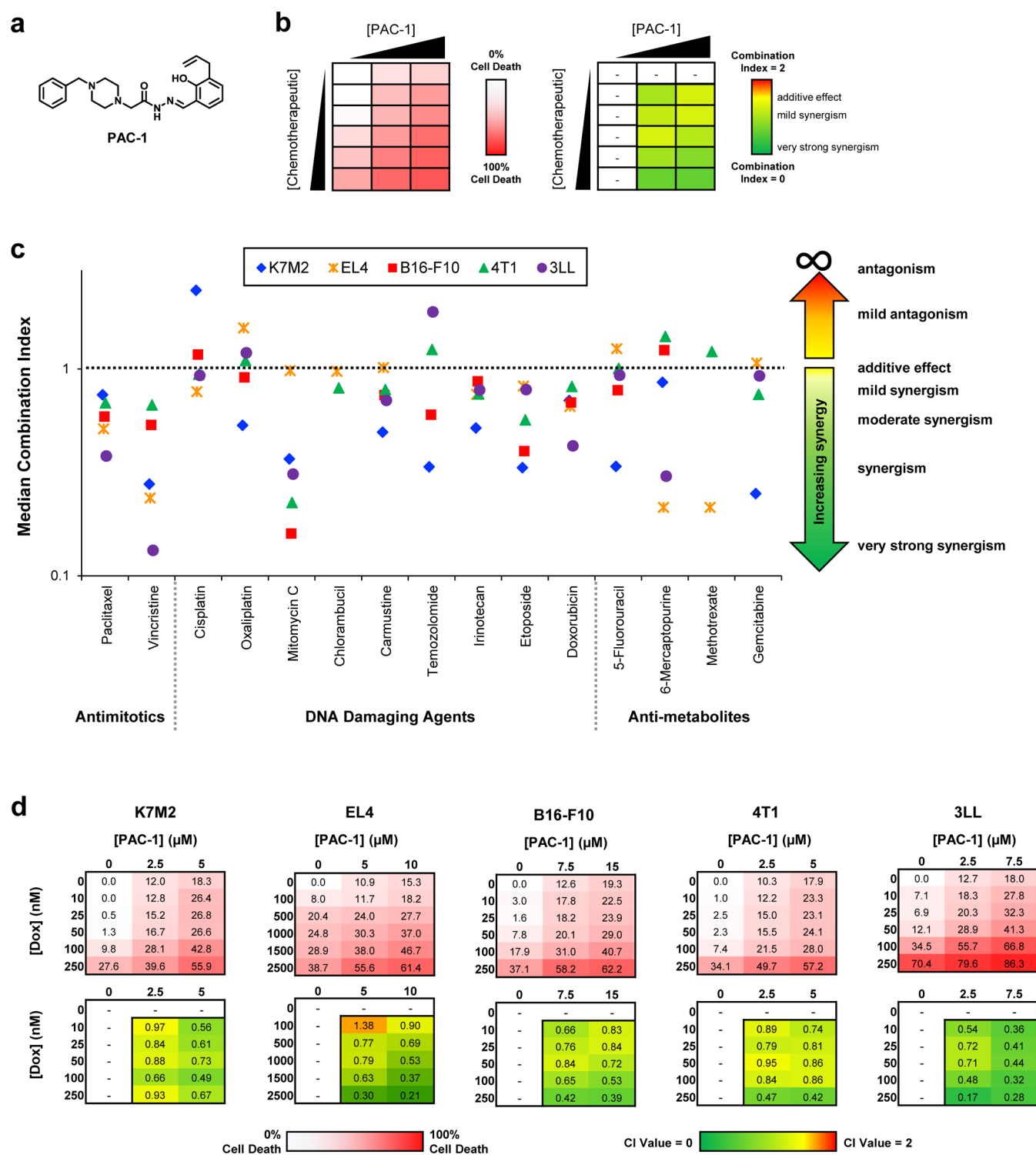


Figure 1. PAC-1 exhibits broad synergy with conventional chemotherapeutics in procaspase-3 overexpressing cell lines. (a) Structure of PAC-1. (b) Schematic of treatment of cancer cells in culture with matrix combinations of PAC-1 plus approved chemotherapeutics. For each cell line, each of 15 chemotherapeutics was evaluated for the ability to induce cell death at 6 concentrations in combination with three concentrations of PAC-1. The CI value was calculated for cell death induced by each PAC-1 + chemotherapeutic combination (10 CI values per cell line, per chemotherapeutic). (c) Median CI values for each PAC-1/chemotherapeutic combination for each cell line. CI values < 1 are synergistic, with lower values indicating higher levels of synergy. CI values = 1 indicate an additive effect. CI values > 1 are antagonistic, with high values indicating higher levels of antagonism. CI values range from 0 to infinity. (d) Results of the average cell death induced by PAC-1 + doxorubicin combinations evaluated in the 3 × 6 matrix, and corresponding quantification of synergy with CI values ($n \geq 3$ biologic replicates).

The overexpression of procaspase-3 represents a common alteration in cancer cells that can be exploited therapeutically. Procaspase-3 overexpression has been observed in lympho-

mas,¹⁵ melanoma,¹⁶ lung¹⁷ and breast cancers,¹⁸ among many others.¹⁹ Procaspase-3 is the zymogen form of caspase-3, a key executioner of apoptosis and responsible for the cleavage of

over a hundred cellular proteins.²⁰ During apoptosis, the proteolytic activation of procaspase-3 to caspase-3 dramatically increases the activity of the enzyme.^{21,22} As unrestricted caspase-3 activity is lethal to cells, mechanisms exist that directly inhibit both procaspase-3 activation and caspase-3 activity, including protein inhibitors of caspase-3 (XIAP and survivin) and the labile zinc pool.^{23–25} Labile zinc colocalizes with procaspase-3 within cells^{26,27} and inhibits both procaspase-3²⁸ and caspase-3 activity.^{25,29,30} Procaspase-activating compound 1 (PAC-1) (Figure 1a) is a small-molecule anticancer agent that functions by chelating labile inhibitory zinc from procaspase-3,³¹ thereby facilitating the autoactivation of procaspase-3 to caspase-3.²⁸ This mechanism of PAC-1 has been demonstrated in many different ways,¹⁹ including studies examining the timing of apoptotic events,^{32,33} and experiments using selective caspase inhibitors³² and substrates.³⁴ As a single agent, PAC-1 displays considerable anticancer activity,¹⁹ inducing apoptosis in cell culture and inhibiting tumor growth in murine models, and a derivative demonstrated activity in canine patients with naturally occurring lymphomas.^{33,35} Furthermore, in select studies, PAC-1 has shown the ability to potentiate targeted agents^{36–38} and a limited number of conventional chemotherapeutics (paclitaxel, cisplatin).^{39,40} PAC-1 is currently being administered to cancer patients in a Phase I clinical trial (NCT02355535).

On the basis of its procaspase-3 activating mode of action, lack of toxicity to normal cell types,³² and tolerability in animals,⁴¹ we hypothesized that PAC-1 would enable ubiquitous synergy with diverse cytotoxins in a range of cancer types without additional toxicity. As described herein, PAC-1 potently synergizes with a broad array of cancer drugs in numerous cancer cell types. The combination of PAC-1 and doxorubicin is particularly effective, demonstrating synergy in cell culture and in mouse models of osteosarcoma and lymphoma. The utility of this combination, in the form of both feasibility and activity, was further examined in pet dogs with late-stage metastatic osteosarcoma and lymphoma. In these canine cancer patients, the PAC-1/doxorubicin combination induces significant regression of macro-metastatic lesions in a number of cases. This ability to synergize with conventional chemotherapeutics without inducing additional toxicity suggests broad potential for PAC-1 as an add-on to standard-of-care cytotoxic anticancer regimens.

RESULTS

PAC-1 Increases the Potency of Diverse Chemotherapeutics in Procaspase-3 Overexpressing Cells. The ability of PAC-1 to induce cell death in combination with common cytotoxic chemotherapeutics was assessed in a matrix format in five diverse solid and hematopoietic cancer types (osteosarcoma, lymphoma, melanoma, breast cancer, and lung cancer) that are commonly treated with such cytotoxic drugs. The 3 × 6 matrices (schematic in Figure 1b) were designed such that two PAC-1 concentrations induced ~10 to 20% cell death during the 24-h treatment, whereas five concentrations for chemotherapeutic agents induced up to 50% cell death. The Chou–Talalay method⁴² was used to quantify the effects, and combination index (CI) values were calculated for each combination, resulting in 10 CI values per chemotherapeutic agent (schematic in Figure 1b). Murine cancer cell lines (K7M2, EL4, B16-F10, 4T1, and 3LL) representing each of the five cancer types were used for these initial experiments, as a prelude to the *in vivo* syngeneic models

(below), and the most promising combinations were further evaluated in human cancer cell lines. As is true with most cancer cell lines, these murine cell lines have a robust expression of procaspase-3 (Supporting Figure 1).

The quantification of the combination experiments is depicted in Figure 1c, with median CI values shown for each PAC-1 drug combination (CI values for the entire matrix are shown in Supporting Information Figure 2). CI values < 1 indicate a synergistic interaction, with lower values demonstrating stronger synergy.⁴² As shown in Figure 1c, PAC-1 synergizes with many different cytotoxins to potently induce death in these cell types; combinations with paclitaxel, vincristine, mitomycin C, carmustine, irinotecan, etoposide, and doxorubicin were particularly effective across all cancer types. Although many of these combinations are intriguing and potentially useful, the combination of PAC-1 and doxorubicin was selected for further investigation, as doxorubicin is a widely used anticancer drug, this combination displays uniformly low CI values, and the PAC-1/doxorubicin combination is capable of inducing high levels of death across the five cancer cell lines (Figure 1d; see Supporting Figure 2a–e for complete combination data).

PAC-1 and Doxorubicin Combinations Show Broad Synergistic Activity against Cancer Cells in Culture.

Doxorubicin is an anthracycline natural product widely used as both a single agent and as the backbone of many combination chemotherapy regimens. It is included in the World Health Organization List of Essential Medicines and is commonly used to treat a variety of cancers, including leukemias, lymphomas, osteosarcomas, soft tissue sarcomas, and cancers of the breast, lung, and ovaries.^{43,44} The diverse cancers for which doxorubicin has demonstrated activity, coupled to the overexpression of procaspase-3 in these cancers, suggests that synergistic PAC-1 and doxorubicin combinations would possess broad clinical utility. The proapoptotic activity of doxorubicin is due to its ability to intercalate DNA, as well as bind topoisomerase II (Top2), stabilizing the ternary Top2-doxorubicin-DNA cleavage complex and thereby inhibiting the process of replication.⁴⁵ Unfortunately, treatment with doxorubicin is accompanied by significant toxicity in the form of cardiomyopathy, which can lead to congestive heart failure. This is due to the ability of doxorubicin to inhibit the cardiomyocyte-specific Top2 β isoform, leading to apoptosis and the generation of reactive oxygen species.⁴⁶ In order to attenuate the risk of congestive heart failure, a maximum lifetime cumulative dose of 400–450 mg/m² for adults is recommended.⁴⁴ The challenge of exploiting the anticancer activity of doxorubicin, while minimizing the risk for cardiac toxicity, has spurred the creation of the field of cardio-oncology,⁴⁷ as well as development of methods to predict patients most likely to experience doxorubicin-induced cardiomyopathy.⁴⁸ Identification of a molecularly targeted agent that could increase the *in vivo* activity of doxorubicin without compounding the associated toxicity would significantly increase the clinical utility of this indispensable chemotherapeutic.

The panel of five cancer cell lines treated with combinations of PAC-1 and doxorubicin demonstrated significantly enhanced cell death at multiple concentrations in the 3 × 6 matrix (Figure 1d). This combination was further examined in each murine cell line and two human cell lines for each cancer type, evaluating the agents in expanded 8 × 8 matrices. As shown in Figure 2a, the PAC-1/doxorubicin combination induces highly

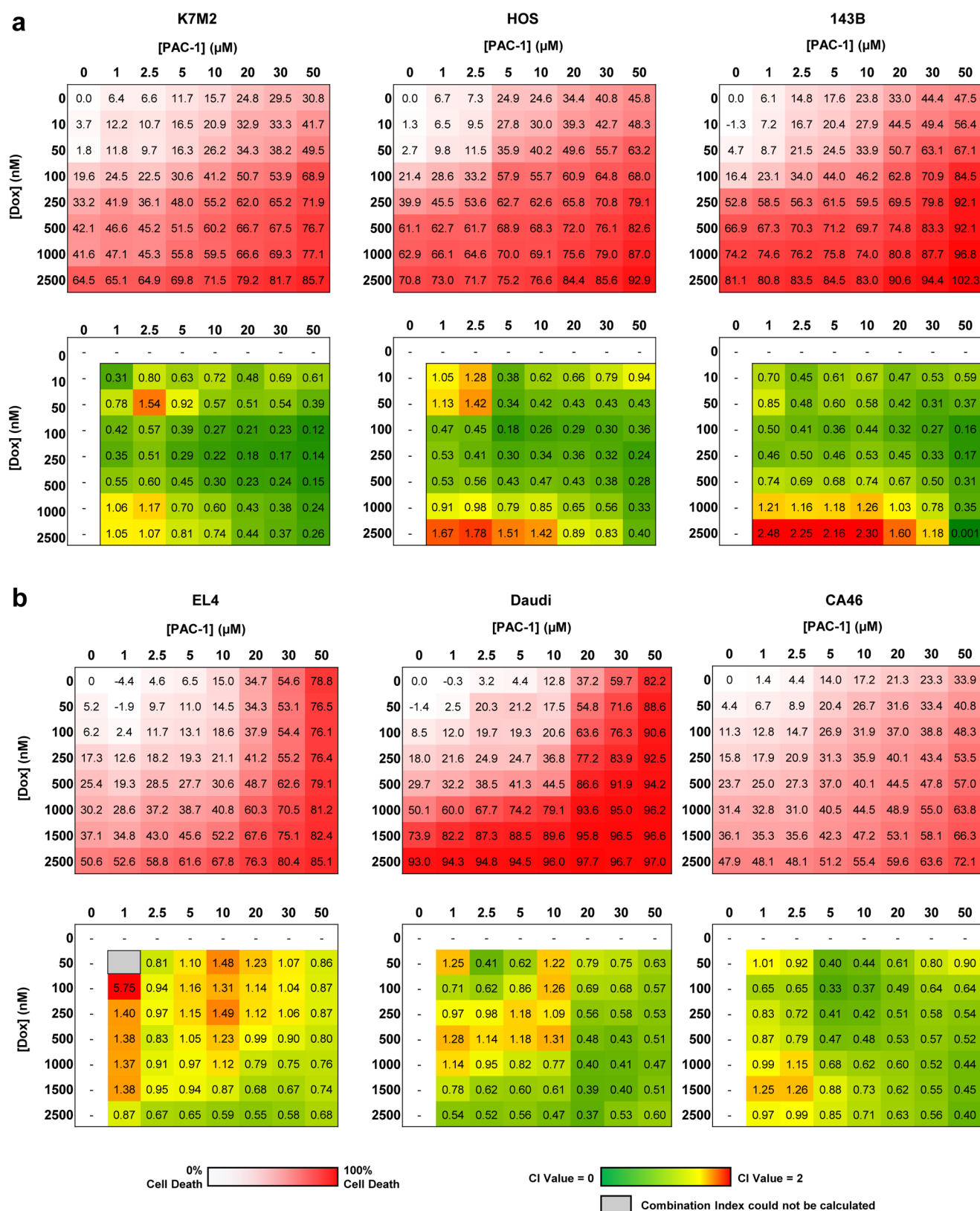


Figure 2. Combination of PAC-1 and doxorubicin shows strong synergistic cytotoxic activity in cancer cells in culture. The average cell death and CI value quantification for 8×8 matrices of PAC-1 and doxorubicin in murine and human osteosarcoma (a) and lymphoma (b) cell lines ($n \geq 3$ biologic replicates). See Supporting Figure 3 for 8×8 matrix combinations of PAC-1 and doxorubicin in melanoma, breast cancer, and lung cancer.

synergistic cell death in three osteosarcoma cell lines: K7M2 (murine), HOS (human), and 143B (human), as well as three lymphoma cell lines (Figure 2b): EL4 (murine), Daudi

(human), and CA46 (human). Strong synergy was also observed for PAC-1/doxorubicin in 8×8 matrices for melanoma, breast cancer, and lung cancer (three cell lines

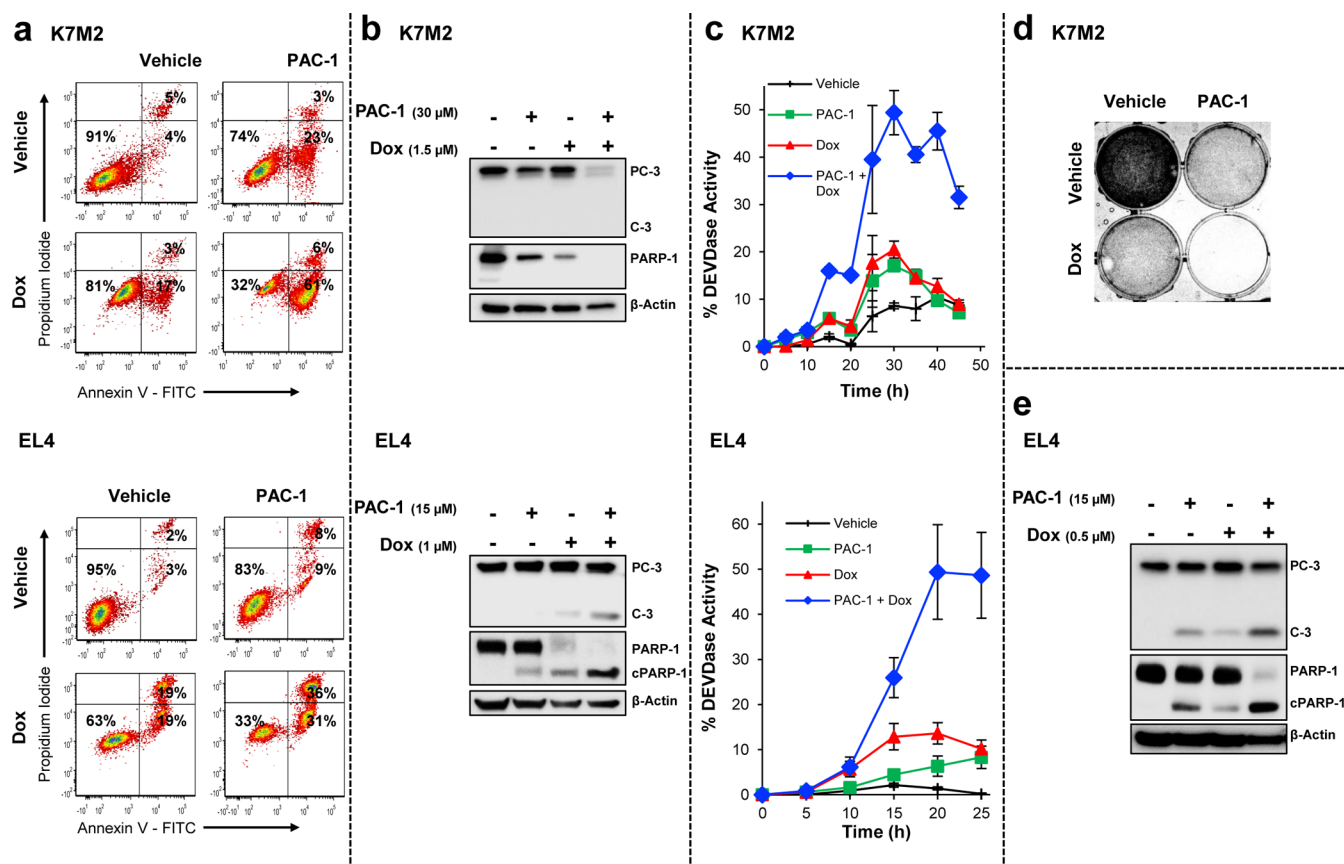


Figure 3. Combination of PAC-1 and doxorubicin induces apoptosis in cancer cell lines. Cancer cell lines K7M2 (top panels) and EL4 (bottom panels) were treated with vehicle, PAC-1 (K7M2:30 μM, EL4:15 μM), doxorubicin (K7M2:1.5 μM, EL4:1 μM), or the combination of PAC-1 + doxorubicin, and evaluated for (a) the induction of apoptosis by Annexin V-FITC and propidium iodide staining (K7M2:48 h treatment, EL4:24 h treatment), by (b) Western blot analysis for cleavage of markers of apoptosis procaspase-3 and PARP-1 (K7M2:48 h treatment, EL4:24 h treatment), and (c) for executioner caspase activity over time. Markers indicate the average executioner caspase activity observed for each time point ($n \geq 3$ biologic replicates, error bars show SEM). (d) Adherent K7M2 cells were stained for qualitative comparison of biomass following treatment for 48 h. (e) Western blot analysis (from EL4 cells) for cleavage of procaspase-3 and PARP-1, with cells treated with a reduced concentration (0.5 μM) of doxorubicin (20 h treatment). Annexin V-FITC/propidium iodide plots, Western blots, and caspase activity time course evaluations are representative of at least three independent biologic experiments. See Supporting Figure 5 for analogous evaluations of PAC-1 and doxorubicin in melanoma, breast cancer, and lung cancer. Western blot in panel e is also shown in Supporting Figure 6.

each, see Supporting Figure 3). A wide range of concentrations of both doxorubicin and PAC-1 were chosen to investigate whether PAC-1 would synergize with doxorubicin regardless of the strength of pro-apoptotic assault provided by doxorubicin, as well as to enhance the biologic significance of calculated CI values.

A second combination identified in the initial experiments was further investigated. The combination of PAC-1 and mitomycin C was explored in osteosarcoma, melanoma, and breast and lung cancer cell lines (three cell lines for each cancer type, Supporting Figure 4). Mitomycin C induces apoptosis through the cross-linking of complementary strands of DNA.⁴⁹ Although it was approved in 1974 for the treatment of cancers of the head and neck, lungs, breast, cervix, colon, hepatic cell carcinoma, melanoma, stomach and pancreatic cancer, these indications were revised in 1975 to only include use in advanced gastric and pancreatic cancers due to inconsistent activity and unacceptable levels of toxicity.⁵⁰ As such, the ability of a well-tolerated small molecule to improve mitomycin C activity in the absence of compounding toxicity could be of high clinical importance. Consistent with the expanded evaluation of PAC-1/doxorubicin combinations, the combination of PAC-1 and mitomycin C was found to be strongly

synergistic across a broad range of concentrations and cell lines (Supporting Figure 4).

The synergistic effect and mode of cell death induced by the PAC-1/doxorubicin combination were further assessed for apoptosis (by flow cytometry, Figure 3a and Supporting Figure 5a) and for activation of procaspase-3 and cleavage of PARP-1 by Western blot (Figure 3b and Supporting Figure 5b) and caspase activity assay (Figure 3c and Supporting Figure 5c). The remaining cellular biomass following the treatments analyzed for apoptosis by flow cytometry and Western blot was visualized by cell fixation and stained with sulforhodamine B (Figure 3d and Supporting Figure 5d). Treatment of the osteosarcoma (Figure 3a, top) or lymphoma (Figure 3a, bottom) cell lines with the PAC-1/doxorubicin combination followed by Annexin V/PI staining reveals marked synergy, with the majority of cells Annexin V positive and PI negative, indicative of apoptosis; similar results are seen in the breast, lung, and melanoma cell lines (Supporting Figure 5a). Western blot analysis of osteosarcoma and lymphoma cells after PAC-1/doxorubicin treatment reveals cleavage of procaspase-3 and PARP-1 (Figure 3b), with similar results observed in the breast, lung, and melanoma cell lines (Supporting Figure 5b). Analysis of caspase-3/-7 activity of treated cells over time indicates that

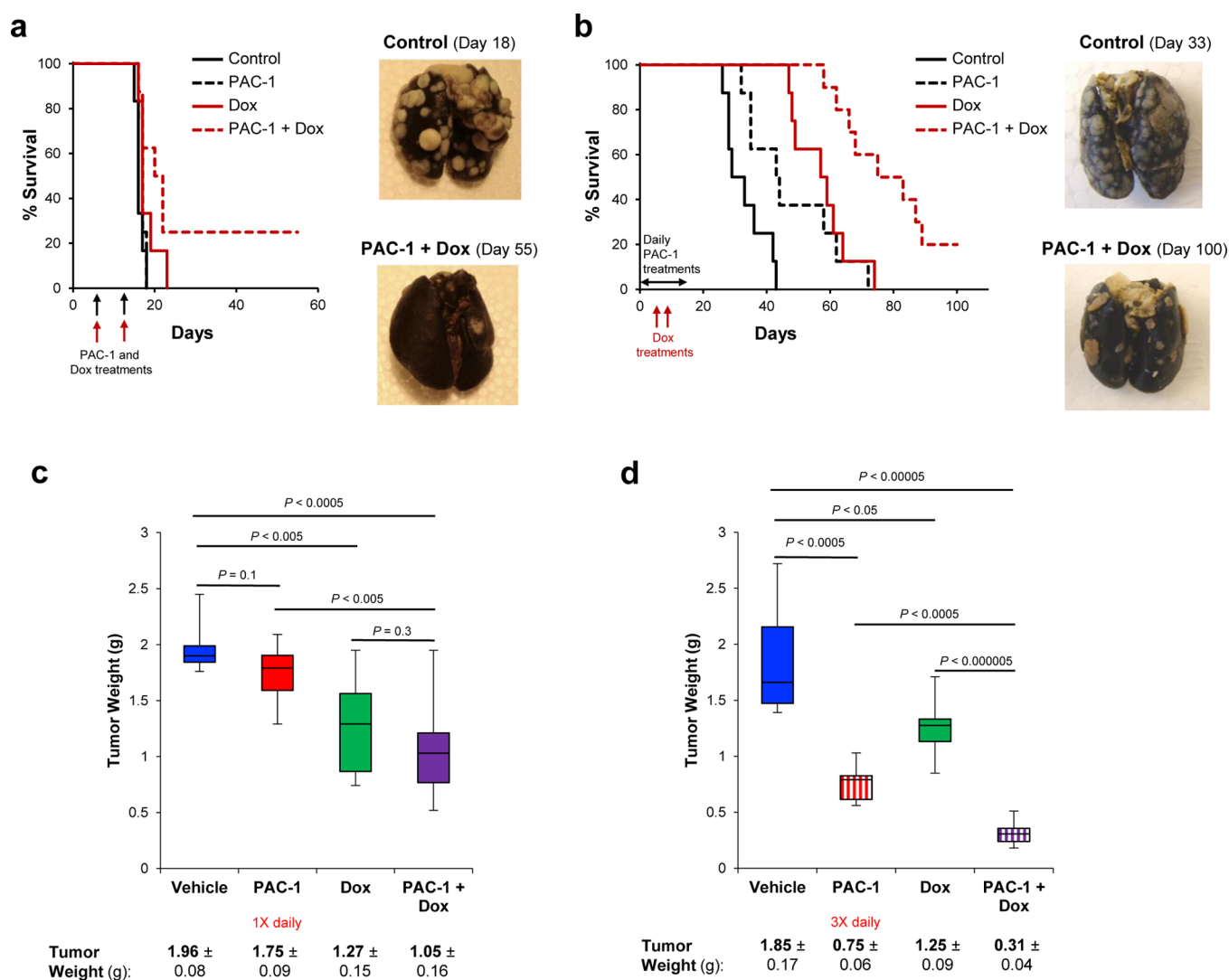


Figure 4. Combination of PAC-1 and doxorubicin has efficacy in murine tumor models. PAC-1, doxorubicin, and PAC-1 + doxorubicin were evaluated in a metastatic syngeneic K7M2 murine osteosarcoma model (a, b) and in a syngeneic subcutaneous EL4 murine lymphoma model (c, d). (a) Experimental metastatic K7M2 cancer was initiated in BALB/c mice via tail vein injection of 1 million K7M2 cells and inoculated mice were treated with PAC-1 (days 7 and 14, 100 mg/kg, oral, in HP β CD), with doxorubicin (days 7 and 14, 5 mg/kg, IV, in 0.9% saline) or with vehicles. Remaining mice were sacrificed after 55 days. $n = 8$ mice per group. Stained lungs from vehicle and PAC-1 + doxorubicin treated animals demonstrate substantial differences in tumor burden. (b) K7M2 inoculated mice were treated with PAC-1 (daily from days 1–15, 125 mg/kg, oral, in HP β CD), with doxorubicin (days 5 and 10, 7.5 mg/kg, IV, in 0.9% saline) or with vehicles. $n = 8–10$ mice per group. Stained lungs from vehicle and PAC-1 + doxorubicin treated animals demonstrate substantial differences in tumor burden. (c) Subcutaneous EL4 lymphoma tumors were established in C57BL/6 mice (5 million cells per mouse) and inoculated mice were treated with PAC-1 once-a-day (days 1–9, 100 mg/kg, IP, in HP β CD), with doxorubicin (days 3 and 7, 7.5 mg/kg, IP, in 0.9% saline) or with vehicles. After 10 days the mice were sacrificed and the tumors excised and weighed. $n = 8$ mice per group. (d) EL4 inoculated mice were treated with PAC-1 thrice-daily (days 1–9, 100 mg/kg, IP, in HP β CD), with doxorubicin (days 3 and 7, 7.5 mg/kg, IP, in 0.9% saline) or with vehicles. After 10 days the mice were sacrificed and the tumors excised and weighed. $n = 7–8$ mice per group. EL4 tumor growth curves and image of extracted tumors in Supporting Figure 8.

cotreatment with PAC-1 greatly increases the extent to which a given concentration of doxorubicin is capable of activating executioner caspases (Figure 3c and Supporting Figure 5c). Importantly, complementary investigations by Western blot for executioner caspase activity, as measured by the time-dependent cleavage of the endogenous substrate PARP-1, demonstrate that the mechanisms of action of doxorubicin, an intrinsic pathway activator, and PAC-1, a direct procaspase-3 activator, do not change dramatically when the agents are used in combination (Supporting Figure 6). In the presence of PAC-1, doxorubicin-induced apoptosis generates higher levels of executioner caspase activity, as measured with the peptidic substrate (Figure 3c and Supporting Figure 5c), as well as near-

quantitative cleavage of PARP-1 even at low concentrations of doxorubicin, as compared to the minimal PARP-1 cleavage in the absence of PAC-1 (Figure 3e). A structurally related but inactive PAC-1 analogue (called PAC-1a)²⁸ was unable to potentiate doxorubicin (Supporting Figure 7), further supporting the importance of procaspase-3 activation to this synergy.

The PAC-1/Doxorubicin Combination Is Effective in Murine Models of Osteosarcoma and Lymphoma. The PAC-1/doxorubicin combination was evaluated in syngeneic murine models of osteosarcoma and lymphoma. The first model investigated was an osteosarcoma experimental metastases model, with the K7M2 murine cell line, with survival as an experimental end point. This model enables evaluation of

the PAC-1/doxorubicin combination in the setting of microscopic metastatic disease. The K7M2 model results in numerous metastases to the lungs, representative of human disease progression and metastasis.⁵¹ In this model two different dosing strategies were evaluated, enabling evaluation of minimal dosages not expected to be effective as single agents, and more frequent dosing, predicted to be moderately effective. In the first experiment, mice were treated with vehicles, PAC-1 (100 mg/kg, oral, on days 7 and 14), doxorubicin (5 mg/kg, IV, on days 7 and 14), or the combination. As predicted, and shown in Figure 4a, PAC-1 and doxorubicin were not effective as single agents under these conditions, but the combination extends the median survival, with 25% of mice surviving until the end of the experiment. After 55 days, the surviving mice were sacrificed, and the lungs were examined for tumor nodules. As shown in Figure 4a, pulmonary metastases were clearly visible in vehicle control mice sacrificed on day 18, and markedly fewer lesions were observed in the lungs of the long-term survivors from the combination treatment.

In the second metastatic K7M2 model, the ability of daily PAC-1 treatments to improve survival was evaluated as a single agent and in combination with doxorubicin. As seen in Figure 4b, when mice were treated with PAC-1 as a single agent (125 mg/kg, PO, daily from days 1–15), a significant extension in median survival was observed, from 31 to 43.5 days ($P = 0.02$, compared to vehicle). As a single agent, slightly higher doses of doxorubicin than those used previously (7.5 mg/kg, IV, days 5 and 10) also extended median survival, from 31 to 58 days ($P = 0.0002$ compared to vehicle). When mice were treated with both PAC-1 and doxorubicin, a further increase in median survival was observed to 79 days ($P < 0.0001$, compared to vehicle; $P = 0.002$, compared to doxorubicin) with 20% of mice surviving to study termination at 100 days. Pulmonary metastases were clearly visible in vehicle control mice sacrificed on day 33, and markedly fewer lesions were observed in the lungs of the long-term survivors from the combination treatment upon sacrifice at day 100.

The PAC-1/doxorubicin combination was also evaluated in a subcutaneous syngeneic model of lymphoma, using the EL4 cell line. Tumor-bearing mice were treated with vehicle, PAC-1 as a single agent (100 mg/kg, IP, daily for 9 days), doxorubicin as a single agent (7.5 mg/kg, IP, on days 3 and 7), or the combination of PAC-1 and doxorubicin. Mice were sacrificed 10 days following tumor cell inoculation, when the caliper measurements of the tumors on vehicle-treated mice exceeded 1500 mm³. Upon sacrifice, tumors were extracted and weighed (Figure 4c, see Supporting Figure 8a for tumor volume calculated from caliper measurements over time). Vehicle-treated mice bore an average tumor burden of 1.96 ± 0.08 g, whereas the PAC-1 treatment group trended toward modestly smaller tumors at 1.75 ± 0.09 g ($P = 0.1$, compared to vehicle). Treatment with doxorubicin significantly reduced tumor burden by approximately a third to 1.27 ± 0.15 g ($P < 0.005$, compared to vehicle). Co-treatment with PAC-1 and doxorubicin further reduced the tumor burden to approximately half of vehicle-treated mice, 1.05 ± 0.16 g ($P < 0.0005$, compared to vehicle).

Recognizing that the half-life of PAC-1 in mice is extremely short, 25 ± 0.9 min, compared to 2.1 ± 0.3 h in dogs,^{41,52} we investigated whether increased frequency of dosing would increase the activity of PAC-1 as a single agent and in combination with doxorubicin; this study served as a prelude for the treatment of canine cancer patients. The EL4

subcutaneous model was repeated, and mice were treated with vehicle, PAC-1 (100 mg/kg, IP, three times daily for 9 days), doxorubicin (7.5 mg/kg, IP, on days 3 and 7), or the combination of PAC-1 and doxorubicin, and tumors were excised on day 10 (Figure 4d, see Supporting Figure 8b,c for tumor volume calculated from caliper measurements over time and images of tumors). Repeated daily dosing significantly improved the activity of PAC-1 as a single agent and in combination with doxorubicin. In this experiment, the tumor size of vehicle and doxorubicin treated mice were consistent with the previous result (Figure 4c), measuring 1.85 ± 0.17 g and 1.25 ± 0.09 g, respectively. Thrice daily dosing with PAC-1 reduced the tumor size to 0.75 ± 0.06 g ($P < 0.0005$, compared to vehicle). The thrice daily dosing of PAC-1 in combination with two treatments with doxorubicin further reduced the tumor burden to 0.31 ± 0.04 g ($P < 0.00005$, compared to vehicle).

The PAC-1/Doxorubicin Combination Induces Tumor Regression in Canine Lymphoma and Metastatic Osteosarcoma Patients and Is Well Tolerated. While murine tumor models enable facile *in vivo* evaluation of potential anticancer drugs and combinations, they frequently fail to predict clinical success in human patient populations. Reasons for this include the abbreviated murine life span, homogeneity of the tumors due to clonal selection in cell line growth, lack of long periods of cancer latency, frequent absence of micro- and macro-metastases, and species differences in drug exposure, among many others.^{53,54} The evaluation of anticancer drugs in pets with spontaneous cancers represents an opportunity to complement induced murine models with naturally occurring cancers. Pet dogs are large mammals, more similar in size and physiology to humans. Many canine cancers are very similar to their human counterparts at the molecular level.^{55,56} For example, canine osteosarcoma has a gene expression profile indistinguishable from human osteosarcoma,^{57–59} and canine lymphomas also possess many similarities to the human disease; dogs typically present with aggressive high-grade multicentric lymphoma, which is similar to human non-Hodgkin lymphoma.⁶⁰ Canine and human lymphomas share similar genetic features, including alterations to MYC, Bcl-2 and RB1 genes.⁶¹

To further assess the potential of PAC-1 as a clinically useful molecularly targeted agent for use in combination with cytotoxic chemotherapeutics, the feasibility and efficacy of the PAC-1/doxorubicin combination were evaluated in canine cancer patients. Canine patients with measurable metastatic osteosarcoma are typically treated with either doxorubicin or a platinum drug (cisplatin or carboplatin), but with minimal efficacy: partial responses are observed in only 5% of patients.^{59,62} Canine lymphoma patients are typically treated with the CHOP protocol or with doxorubicin as a single agent. These treatments are more effective; 7–10 month remissions and survival of greater than one year are observed in approximately 50% of patients.⁶³ The expression of procaspase-3 in canine lymphomas has been previously noted in lymph node aspirates taken from canines with both T-cell and B-cell lymphomas.³⁵ As a prelude to our clinical study, the presence of the procaspase-3 target was analyzed in canine osteosarcoma, and the data reveal that procaspase-3 is overexpressed in malignant canine osteoblasts compared to normal osteoblasts (Supporting Figure 9).

PAC-1/Doxorubicin in Canine Osteosarcoma. Evaluation of PAC-1 plus doxorubicin was initiated in canines with

Table 1. Canine Metastatic Osteosarcoma Patients Treated with High Dose Oral PAC-1 + Dox^a

patient	breed	sex	age (y)	weight (kg)	location of primary tumor	metastases	prior therapy	treatment ^b		outcome
								PAC-1 (mg/kg)	Dox ^c (mg/m ²)	
1	Labrador retriever	FS	11	31	L distal femur	pulmonary	PD on carboplatin	50	30	PD
2	Golden retriever	FS	5	37	R proximal humerus	subcutaneous	PD on carboplatin	50	30 (25, 20)	SD
3	Shepherd mix	MC	12	27	L distal ulna	pulmonary	PD on carboplatin	50	30 (25, 25)	PD

^aAbbreviations: FS, female spayed; MC, male castrated; L, left; R, right; PD, progressive disease; SD, stable disease; PR, partial response. ^bPAC-1 (oral tablet) was administered 4 h prior to treatment with doxorubicin (IV bolus). This treatment was repeated every 14 days, for ≥ 3 cycles. Patients 1 and 3 received three treatment cycles. Patient 2 received a total of nine cycles of PAC-1 + dox treatments. Treatments 4–9 occurred with the dox dosage given in the third treatment (20 mg/m²). ^cValues in parentheses indicate dosage of dox for second and third treatment.

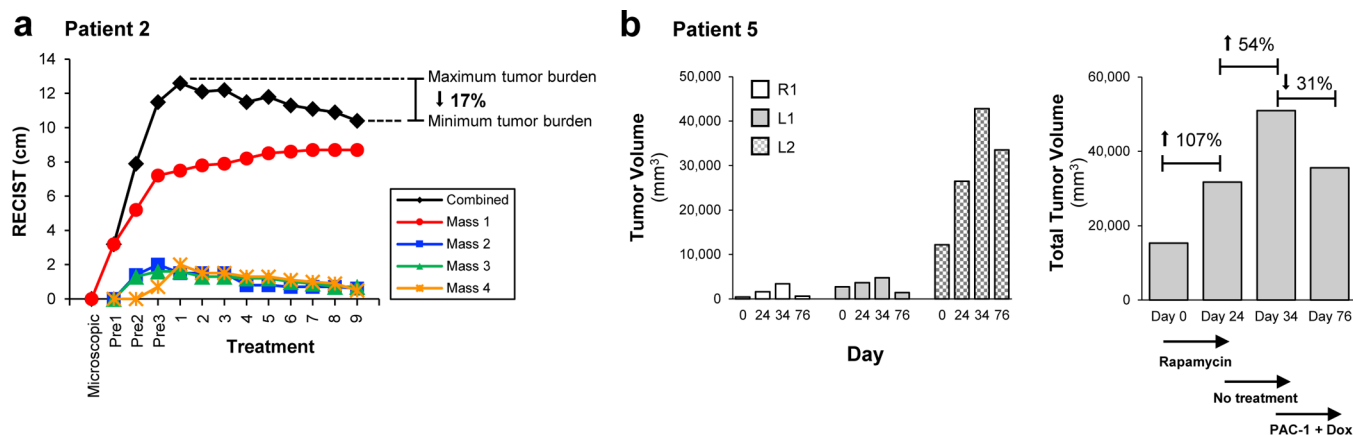


Figure 5. Combination of PAC-1 and doxorubicin is well tolerated and has efficacy in canine patients with naturally occurring metastatic osteosarcoma (a) A pet dog (Patient 2) presented with rapidly growing, carboplatin-resistant osteosarcoma, with four measurable masses. Patient 2 was treated with 50 mg/kg PAC-1 (oral), followed by 20–30 mg/m² doxorubicin (IV) 4 h later. Treatments were administered every 14 days, for 9 cycles. (b) A pet dog (Patient 5) presented with rapidly growing, rapamycin-resistant osteosarcoma, with three measurable lung masses (denoted as R1, L1, and L2). Patient 5 was treated daily with 12.5 mg/kg PAC-1 (oral, 42 consecutive days), and 25 mg/m² doxorubicin on days 34, 48, and 62.

Table 2. Canine Metastatic Osteosarcoma Patients Treated with Metronomic Oral PAC-1 + Dox^a

patient	breed	sex	age (y)	weight (kg)	location of primary tumor	metastases	prior therapy	treatment ^b		outcome
								daily PAC-1 (mg/kg)	Dox (mg/m ²)	
4	Labradoodle	MC	8	36	L proximal tibia	pulmonary	naïve	10.9–11.5	25	PR
5	Mixed breed	MC	6	22	L distal radius	pulmonary	PD on rapamycin	12.5	25	PR
6	Golden retriever	MC	9	32	R 9th rib	pulmonary	PD on carboplatin	12.5	25	PD

^aAbbreviations: MC, male castrated; L, left; R, right; PD, progressive disease; PR, partial response. ^bPAC-1 (oral tablet) was administered daily for 6 weeks. Doxorubicin (IV bolus) was given every 14 days, for a total of 3 doses.

naturally occurring measurable metastatic osteosarcoma. Pet dogs presented at or referred to the Small Animal Clinic at the University of Illinois at Urbana–Champaign College of Veterinary Medicine were considered for enrollment in the clinical trial (see [Materials and Methods](#) for inclusion criteria). PAC-1 (oral tablet) at single doses of 50, 100, and 200 mg/kg was well tolerated in healthy research dogs, and doses of 25 mg/kg (oral tablet) once-a-day for at least 84 days (21 consecutive days followed by a seven day wash out period, repeated for three cycles) were also well tolerated. As such, treatment of the first cohort of patients (Table 1, Patients 1–3) was initiated at a 50 mg/kg PAC-1 (PO) dosage, followed by 20–30 mg/m² doxorubicin (IV) 4 h later. Both drugs were administered once every 2 weeks, with all animals receiving at least three treatment cycles. Patients 2 and 3 required a dose reduction from 30 mg/m² doxorubicin after presenting with grade 2 or greater gastrointestinal distress, believed to be due to doxorubicin. Although doxorubicin dosages ≤ 20 mg/m² are

considered subtherapeutic, they were evaluated for activity based upon the profound synergy observed between PAC-1 and doxorubicin in cell culture and murine models. Because of overall disease stabilization and reduction in the size of small lesions, Patient 2 continued to receive the PAC-1/doxorubicin combination treatment for nine cycles. As shown in Figure 5a, Patient 2's tumors were rapidly progressing when treated with carboplatin (microscopic and Pre1–3 RECIST scores). Overall tumor growth ceased upon treatment with PAC-1 and doxorubicin, with the three smaller lesions (Masses 2–4) decreasing in size over the course of treatment. Growth of the largest lesion (Mass 1) stabilized, resulting in an overall 17% reduction in total tumor burden and RECIST categorization of stable disease.

Because an increased frequency in PAC-1 dosing led to an increase in anticancer efficacy in the murine models, the feasibility of treating patients with lower doses of oral PAC-1 daily in combination with biweekly IV treatments of

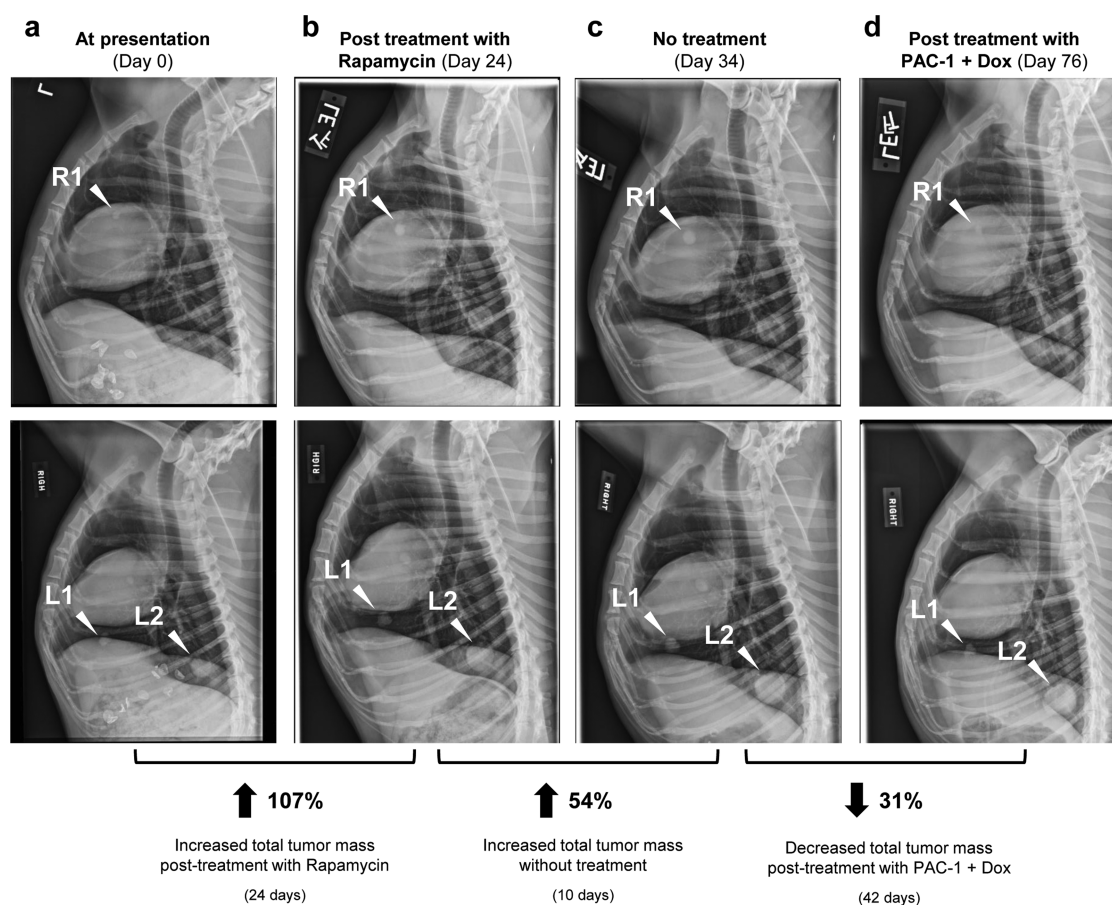


Figure 6. Activity of PAC-1 + doxorubicin against metastatic osteosarcoma in Patient 5. Chest films of masses R1, L1, and L2 at presentation (a), post treatment with rapamycin (b), 10 days without treatment (c), and post treatment with PAC-1 + doxorubicin (d). Quantification of mass size in Figure 5b.

Table 3. Canine Lymphoma Patients Treated with High Dose Oral PAC-1 + Dox^a

patient	breed	sex	age (y)	weight (kg)	prior therapy	treatment ^b		outcome
						PAC-1 (mg/kg)	Dox (mg/m ²)	
7	Golden retriever	MC	7	45	naïve	75	30	PR
8	Golden retriever	FS	6	44	naïve	75	30	CR
9	Mixed breed	MC	14	22	naïve	75	30	CR
10	Golden retriever	MI	11	39	naïve	100	30	PR

^aAbbreviations: FS, female spayed; MC, male castrated; MI, male intact; PR, partial response; CR, complete response. ^bPAC-1(oral tablet) was administered 4 h prior to treatment with doxorubicin (IV bolus). This treatment was repeated every 14 days, for three cycles.

doxorubicin was explored. Three patients were treated daily with PAC-1 (10–12.5 mg/kg oral tablet, or approximately 1/10th of the highest oral dosage of PAC-1, evaluated in Patient 10) and doxorubicin (25 mg/m² IV on days 1, 14, and 28) (Table 2, Patients 4–6). Patient 4, a drug naïve osteosarcoma patient, presented with three macro-metastases in the lungs; 2 of 3 lesions decreased in size following treatment with PAC-1 + doxorubicin (see Supporting Figure 10 for tumor size quantification and chest films). Patient 5 was admitted to the study with progressive measurable osteosarcoma metastases following treatment with oral rapamycin. All three of Patient 5's lesions decreased in size with treatment of PAC-1 and doxorubicin (see Figure 5b for quantified tumor measurements and Figure 6 for chest films of lesions).

PAC-1/Doxorubicin in Canine Lymphoma. The combination of PAC-1 and doxorubicin was also evaluated in canines with naturally occurring lymphomas (Table 3, Patients 7–10).

As canine lymphomas are commonly treated with the CHOP therapy regimen and doxorubicin is known to be efficacious as a single agent,⁶⁴ the main priority of these studies was to further confirm the feasibility of combining PAC-1 (oral) with doxorubicin (IV) in canine lymphoma patients. Upon the basis of the tolerability of 50 mg/kg PAC-1 observed in the osteosarcoma patients, the feasibility of an increased dose was evaluated in three patients who received PAC-1 (75 mg/kg PO), followed by doxorubicin (30 mg/m², IV) 4 h later. Complete responses were observed in 2/3 patients, with Patient 7 demonstrating a partial tumor regression. A fourth canine lymphoma patient, Patient 10, was treated with PAC-1 (100 mg/kg PO) and doxorubicin (30 mg/m², IV), with the treatment being well tolerated, and a partial response was observed.

Tolerability of PAC-1/Doxorubicin Treatment in Mice and Dogs. A significant objective of these experiments was to

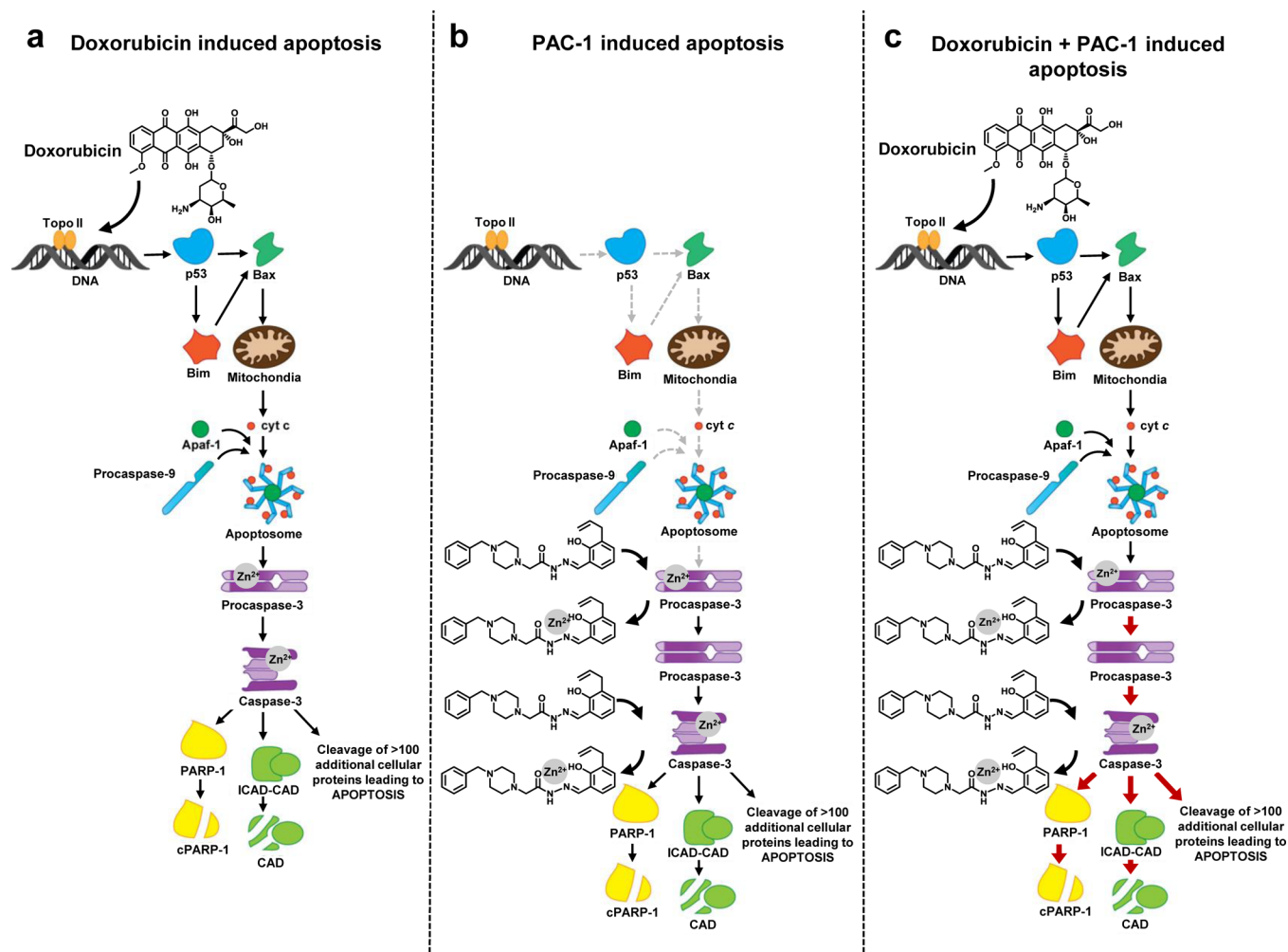


Figure 7. PAC-1 enhances the apoptotic signal as induced by cytotoxins such as doxorubicin. (a) Doxorubicin inhibits topoisomerase II, resulting in canonical intrinsic pathway apoptosis. (b) PAC-1 induces apoptosis through chelation of labile inhibitory zinc from procaspase-3, and PAC-1 also relieves zinc-mediated inhibition of caspase-3 activity. (c) The combination of PAC-1 and doxorubicin induces amplified levels of apoptosis due a primed (nonzinc inhibited) population of procaspase-3 that is more responsive to upstream proteolysis (see data in Figure 3b and Supporting Figures 5b and 6). In addition, PAC-1 enables any caspase-3 generated by doxorubicin to be more active, through chelation of inhibitory zinc from caspase-3 (see data in Figure 3c and Supporting Figure 5c). Elevated caspase-3 activity leads to enhanced cleavage of the endogenous protein substrate PARP-1 (Figure 3b,e and Supporting Figures 5b and 6), and higher levels of apoptotic cell death (Figure 3a and Supporting Figure 5a).

assess the tolerability of the PAC-1/doxorubicin combination *in vivo*. Of particular interest was to determine whether PAC-1 cotreatment would compound the cardiomyopathy induced by doxorubicin. As the major limitation to patient treatment with doxorubicin is the lifetime cumulative dose limit, in order for a molecularly targeted agent to be suitable for combination it must not induce cardiotoxicity as a single agent, or increase the toxicity induced by doxorubicin.

To experimentally examine the cardiotoxicity of PAC-1 and doxorubicin treatments, mice were treated with PAC-1 as a single agent (125 mg/kg, PO, daily from days 1–15), doxorubicin (7.5 mg/kg, IV, days 5 and 10), or the two agents in combination (the dosing scheme used in Figure 4b, K7M2 metastatic osteosarcoma model). As the cumulative dosage of doxorubicin administered in the in the span of a week equaled 15 mg/kg, mice were expected to demonstrate some measurable degree of cardiomyopathy on histopathological evaluation.^{46,65} As expected, treatment with doxorubicin induced a reduction in the average body weight of the cohort (Supporting Figure 11a), but importantly, daily treatments with PAC-1 did not reduce average body weights further. At the

conclusion of treatments, animals were sacrificed, and hearts were stained with hematoxylin-eosin and analyzed semi-quantitatively for the frequency and severity doxorubicin-induced myocardial alterations, scored from 0 (no alteration) to 3 (>35% of myocardial cells showing damage).⁶⁶ As shown in Supporting Figure 11b (quantitation) and 11c and (representative images), no significant difference was observed across treatment groups, demonstrating that cotreatment with daily PAC-1 did not overtly enhance any of the doxorubicin-induced markers of cardiomyopathy.

All canine patients were evaluated for toxicity induced by treatment with oral PAC-1 and IV doxorubicin via serial complete blood counts and serum chemistry panels. The hematologic and biochemical parameters support the feasibility of safely combining the agents. None of the treated dogs showed significant signs of toxicity beyond the expected toxicity of doxorubicin treatments alone (as shown in Supporting Table 1). Additionally, an EKG was performed on all patients immediately prior to each doxorubicin treatment. As the patients received ≥ 3 treatments with doxorubicin, EKG results were obtained 14 days after each treatment (with the exception

of the final treatment with doxorubicin). While there are limitations of EKG as a tool for detecting cardiac disease, the EKG analysis did not show any evidence of cardiac arrhythmias, suggesting that cotreatment with PAC-1 did not overtly enhance doxorubicin-induced cardiomyopathy in canine patients.

DISCUSSION

Cytotoxic drugs retain a major role in the treatment of cancer, even in the era of targeted therapy. This continued reliance on cytotoxins is largely due to the limitations of many molecularly targeted agents, most notably the frequent emergence of rapid resistance; thus, the ability of a molecularly targeted agent to be used in combination with cytotoxic chemotherapeutics is essential for treatment of many cancers. Procaspase-3 is a molecular target overexpressed in numerous cancers and a critical node in the induction of cell death. Described herein is the evaluation of synergy of a procaspase-3 activating compound, PAC-1, in combination with cytotoxic drugs. Marked synergy was observed with diverse classes of chemotherapeutic drugs, and further studies with the PAC-1/doxorubicin combination showed its tremendous promise in cell culture, mouse models, and pet dogs with metastatic osteosarcoma and lymphoma. On the basis of all the data, a view of the apoptotic cell death as induced by each single agent and the combination is shown in Figure 7. Doxorubicin inhibits topoisomerase II, leading to canonical intrinsic pathway apoptosis, whereas PAC-1 activates procaspase-3 and enhances the activity of caspase-3 through chelation of labile inhibitory zinc. In the combination, PAC-1 is able to dramatically enhance the pro-apoptotic signal from doxorubicin, both through chelation of labile zinc from procaspase-3 (thus making it more susceptible to proteolysis/activation) and through chelation of labile zinc from caspase-3 (thus making this enzyme more active).

Excitingly, the PAC-1/doxorubicin combination was only one of many intriguing clinically relevant combinations. When PAC-1 was combined with the antimetabolic agents paclitaxel and vincristine, strong synergy was observed across the five cancer types. Paclitaxel is prescribed extensively in the treatment of metastatic breast cancer, and the ability of PAC-1 to enhance its anticancer activity could be of high clinical relevance. Furthermore, PAC-1 demonstrated strong synergy with less commonly used agents, such as mitomycin C, with strong synergy observed in all four solid tumor types assessed. Revival of these agents in combination with PAC-1 could be particularly useful in patients; it is unlikely that they would have been treated with the drug previously, which should delay or abolish the onset of resistance. As the strong synergy between PAC-1/doxorubicin observed in our cell culture experiments translated into efficacy in murine models of cancer and canine cancer patients, optimism exists that other combinations would translate with similar efficiency into complex and clinically relevant settings.

Osteosarcoma was selected for evaluation of the PAC-1/doxorubicin combination because a significant unmet clinical need exists for the treatment of patients with relapsed or metastatic disease. The current standard of care for the human disease is complete surgical resection, followed by combinatorial chemotherapy based upon methotrexate, doxorubicin and cisplatin (MAP protocol), and results in long-term survival of ~70% of patients.⁶⁷ Despite numerous clinical trials aimed at identifying more effective strategies for the treatment of

osteosarcoma, doxorubicin remains the backbone of the therapy and is believed to be the most effective agent.⁶⁸ Unfortunately, survival of patients with relapsed and metastatic osteosarcoma has remained unchanged over the past 30 years, with an overall 5-year survival rate at 20%.⁶⁹ This is largely due to the challenge of treating recurrent macroscopic metastases in the lungs or other anatomic sites less amenable to surgical resection.

Pulmonary macroscopic metastases also represent a major challenge in the treatment of canine osteosarcoma. Approximately 15% of patients present with these lesions upon diagnosis, although estimations suggest that occult metastatic disease is present in ~90% of dogs at diagnosis.⁷⁰ Canine macro-metastatic lesions are extremely resistant to therapeutic intervention, with a ~5% response rate to conventional systemic chemotherapies. Pulmonary metastases in human patients are similarly challenging to treat, and no standard has been established as an effective second-line chemotherapeutic agent. Thus, strategies that elicit a response in canine patients could also prove useful for human patients with the poorest prognosis. The high response rate for PAC-1/doxorubicin in this setting, especially considering that Patients 1, 2, 3, 5, and 6 had demonstrated progressive disease after treatment with traditional chemotherapeutics immediately prior to treatment with PAC-1/doxorubicin, suggests that this combination could be effective in treating recurrent macroscopic metastatic disease not amenable to surgical resection, an unmet clinical need.

Toxicological assessment of both high-dose intermittent PAC-1 and low-dose metronomic PAC-1 revealed no significant toxicity when used in combination with doxorubicin. Importantly, treatment with the PAC-1/doxorubicin combination did not induce increased myelosuppression relative to doxorubicin alone. This result suggests that PAC-1 may be combined effectively with other clinically useful agents or combination regimes without intensifying toxicity. As doxorubicin is a prominent member of numerous chemotherapy regimens for the treatment of diverse cancers, addition of PAC-1 to treatment protocols for the many cancers that overexpress procaspase-3 deserves further exploration. Furthermore, the risk of doxorubicin-induced cardiotoxicity is known to be enhanced in certain patient populations, including children, the elderly, those with liver disease, those possessing a BRCA2 mutation,⁷¹ concurrent treatment with ionizing radiation or trastuzumab,⁷² among others, substantiating the need to develop well-tolerated agents capable of enhancing the activity of doxorubicin. Additionally, although efforts have been made to predict the susceptibility of a human patient to doxorubicin-based cardiotoxicity,⁷³ complementary methods for veterinary patients to be treated with doxorubicin lag behind.

In conclusion, we have identified PAC-1 plus doxorubicin as a well-tolerated combination that is effective in both murine models of cancer and in canine patients with naturally occurring cancers. Because of the important role of doxorubicin in the treatment of numerous cancers and the widespread overexpression of procaspase-3, we anticipate that the combination will be broadly effective.

MATERIALS AND METHODS

Cell Lines and Reagents. K7M2, EL4, LLC, B16-F10, 4T1, Daudi, CA46, HOS, 143B, H1993, H460, BT-549, MDA-MB-436, and SK-MEL-5 cells were obtained directly from the American Type Culture Collection. UACC-62 cells were obtained from the Developmental Therapeutics Program, National Cancer Institute, NIH (Frederick, MD).

Cells were maintained at low passage number and were cultured in RPMI 1640, DMEM, or EMEM supplemented with 10% fetal bovine serum and 1% penicillin-streptomycin, as specified by ATCC and grown at 37 °C and 5% CO₂. SK-MEL-5 and UACC-62 were authenticated using the PowerPlex16HS Assay (Promega): 15 Autosomal Loci, X/Y at the University of Arizona Genetics Core. Cells were treated with Normocin (Invivogen) prior to use and confirmed to be mycoplasma free.

PAC-1 and PAC-1a were synthesized as previously described.³³ Paclitaxel, cisplatin, chlorambucil, carmustine, etoposide, 5-fluorouracil, 6-mercaptopurine, and gemcitabine were purchased from Sigma-Aldrich. Vincristine, oxaliplatin, and irinotecan were purchased from Selleck. Mitomycin C, Temozolomide, and methotrexate were purchased from Cayman Chemical. Doxorubicin was purchased from OChem Incorporation. Chemotherapeutics, with the exception of cisplatin and gemcitabine, were prepared as 10 mM DMSO stocks, aliquoted, and stored at -20 °C until use. Cisplatin was prepared immediately prior to use in 0.9% saline to a concentration of 2 mM. Gemcitabine was prepared immediately prior to use in 0.9% saline to a concentration of 10 mM.

Immunoblotting. For Western blot analysis one million suspension cells or adherent cells at 75% confluency in six-well plates (150,000 to 300,000 cells) were used. At the conclusion of treatment, the medium and Trypsin-aided detached cells were pelleted, lysed on ice in RIPA buffer (50 mM Tris base, 150 mM NaCl, 1% Triton X-100, 0.5% Na-deoxycholate, 0.1% SDS, pH 7.4, with a 1:100 dilution of Protease Inhibitor Cocktail Set III), and clarified, and protein content was normalized by BCA Protein Assay reagent (Pierce). Samples were denatured (10 min, 95 °C), separated by SDS-PAGE (4–20%), and transferred to a membrane for Western blot analysis. Antibodies for procaspase-3 and caspase-3 (9662), procaspase-9 and caspase-9 (9508), PARP-1 (9542) and β -actin (4970) were purchased from Cell Signaling and used as directed.

Cell Death Survey of PAC-1 Combinations with Classical Chemotherapeutics. All cell death experiments were performed with cells treated in 96-well plates, in 100 μ L total volume, and 1% DMSO. Survey plates were prepared as follows: 49 μ L of complete growth media was added, and then each well received 0.5 μ L of PAC-1 stock solution in DMSO at three concentrations selected to induce between 10 and 20% cell death, and 0.5 μ L of chemotherapeutic stock solution in DMSO at six concentrations, up to but not exceeding 100 μ M. For cisplatin and gemcitabine, chemotherapeutics prepared in 0.9% saline, the volume of complete growth medium was reduced to accommodate a larger volume of chemotherapeutic stock if necessary. A total of 0.5 μ L of DMSO was added to each well to ensure all treatments occurred at 1% DMSO. To each well, 50 μ L of a suspension of cells at 800,000 cells/mL (suspension cells) or 100,000 to 120,000 cells/mL (adherent cells) were plated into the wells, for a final density of 40,000 suspension or 5,000 to 6,000 adherent cells per well, respectively. Additionally, each plate had three wells receiving 1 μ L of the positive death control Raptinal⁷⁴ (final concentration 10 μ M), and three wells receiving 1 μ L of DMSO as a negative control. The plates were incubated at 37 °C with 5% CO₂ for 24 h. At the conclusion of treatment, the plates were analyzed by Alamar Blue. For larger 8 \times 8 matrix evaluations of cell death in murine and human cell lines, similar procedures as described above were used. All cell death experiments were performed with three independent biologic replicates.

Assessment of Apoptosis by Flow Cytometry. The induction of apoptosis was measured by Annexin V-FITC/Propidium iodide staining and flow cytometry. Either 250,000 suspension (EL4) cells or adherent cells at ~75% confluency (150,000 to 300,000 cells) in six-well plates were treated with combinations of PAC-1 and doxorubicin for 24 h (EL4 and 3LL) or 48 h (K7M2, B16-F10, 4T1) at 37 °C, 5% CO₂ (EL4:10 μ M PAC-1, 1 μ M dox; 3LL: 10 μ M PAC-1, 1 μ M dox; K7M2:30 μ M PAC-1, 1.5 μ M dox; B16-F10: 10 μ M PAC-1, 0.75 μ M dox; 4T1:7.5 μ M PAC-1, 1 μ M dox). At the conclusion of treatment, the cells (adherent cells detached with trypsin), medium, and debris were transferred to flow tubes and pelleted via centrifugation (500g for 2 min) and suspended in 450 μ L of Annexin V binding buffer (10 mM HEPES, 2.5 mM CaCl₂, 140 mM NaCl, 0.1% BSA, pH 7.4). Buffer was prepared with dyes such that each sample would receive 3 μ L of FITC-conjugated Annexin V (Southern Biotech 10040-02) and 0.25 μ L of a 1 mg/mL solution of propidium iodide (Sigma). Samples were protected from light and stored on ice until assessment. Cell populations were analyzed on a Becton Dickinson LSR II cell flow cytometer. 10,000 events per sample were recorded.

Western Blot Assessment of Cleavage of Procaspase-3, Procaspase-9, and PARP-1. For Western analysis one million suspension (EL4) or adherent cells at 75% confluency (150,000 to 300,000 cells) in six-well plates were treated with combinations of PAC-1 and doxorubicin for 24 h (EL4 and 3LL) or 48 h (K7M2, B16-F10, 4T1) at 37 °C, 5% CO₂ (EL4:10 μ M PAC-1, 1 μ M dox; 3LL: 10 μ M PAC-1, 1 μ M dox; K7M2:30 μ M PAC-1, 1.5 μ M dox; B16-F10:10 μ M PAC-1, 0.75 μ M dox; 4T1:7.5 μ M PAC-1, 1 μ M dox). At the conclusion of treatment, the medium and trypsin-aided detached cells were pelleted, lysed on ice in RIPA buffer (50 mM Tris base, 150 mM NaCl, 1% TritonX-100, 0.5% Na-deoxycholate, 0.1% SDS, pH7.4, with a 1:100 dilution of Protease Inhibitor Cocktail Set III), and clarified, and protein content was normalized by BCA Protein Assay reagent (Pierce). Samples were denatured, separated by SDS-PAGE (4–20%), and transferred to a PVDF membrane for Western blot analysis of procaspase-3 (Cell Signaling 9662), procaspase-9 (Cell Signaling 9508), and PARP-1 (Cell Signaling 9542). Blots were stripped and reprobed for β -actin (Cell Signaling 4970) as a loading control.

Caspase Activation in Cell Lysate. Cells (10,000 per well) were plated in 96-well plates, allowed to adhere, and incubated with 10 μ M Raptinal,⁷⁴ PAC-1, doxorubicin, or DMSO (final DMSO concentration normalized across wells and <1%) in phenol-red free RPMI media. Cells were treated with the concentrations of PAC-1 and doxorubicin used in the flow cytometry and Western blot analyses for apoptosis (K7M2:30 μ M PAC-1, 1.5 μ M dox; EL4:10 μ M PAC-1, 1 μ M dox; B16-F10: 10 μ M PAC-1, 0.75 μ M dox; 4T1:7.5 μ M PAC-1, 1 μ M dox; 3LL: 10 μ M PAC-1, 1 μ M dox). Plates were assessed for executioner caspase activity via addition of a 4X bifunctional lysis activity buffer (200 mM HEPES, 400 mM NaCl, 40 mM DTT, 0.4 mM EDTA, 1% TritonX-100, 50 μ M Ac-DEVD-AFC). Fluorescence was measured over time for 30 min. Activity is expressed as normalized to the vehicle activity at the earliest time point, and maximal activity is defined as the activity induced by 10 μ M Raptinal at 5 h.

Sulforhodamine B Staining of Biomass of Treated Cells. Adherent cells at 75% confluency (150,000 to 300,000 cells) in six-well plates were treated with combinations of PAC-

1 and doxorubicin for 24 h (3LL) or 48 h (K7M2, B16-F10, 4T1) at 37 °C, 5% CO₂ (3LL: 10 μM PAC-1, 1 μM dox; K7M2:30 μM PAC-1, 1.5 μM dox; B16-F10: 10 μM PAC-1, 0.75 μM dox; 4T1:7.5 μM PAC-1, 1 μM dox). At the conclusion of treatment, the medium and dead cells were removed. Viable cells were washed with PBS and fixed overnight at 4 °C with 10% trichloroacetic acid. The plates were then washed gently with H₂O five times. The plates were allowed to air-dry after which 1 mL of a 0.057% (w/v) sulforhodamine B in a 1% (v/v) acetic acid solution was added to each well for 30 min at room temperature. The plates were gently washed 5 times with 1% (v/v) acetic acid and air-dried. Biomass was visualized with a Bio Rad Gel Doc.

K7M2 Experimental Metastasis Tumor Models. All animal experimental procedures were reviewed and approved by the University of Illinois Institutional Animal Care and Use Committee. 1,000,000 K7M2 cells were prepared in HBSS and intravenously injected into the tail vein of 6–8 week old female BALB/c mice (day 0) in a 200 μL volume. Mice were randomized into four treatment groups: vehicle, PAC-1 alone, doxorubicin alone, and PAC-1 + dox. PAC-1 was formulated in HPβCD (10 mg/mL in 200 mg/mL HPβCD at pH 5.5). Doxorubicin was formulated in 0.9% saline (2 mg/mL). For the low dose model, mice were treated with 100 mg/kg PAC-1 orally, followed 4 h later by 5 mg/kg IV doxorubicin on day 7 and day 14. For the chronic dosing model, mice were treated daily from days 1–15 with 125 mg/kg PAC-1 orally, and with 7.5 mg/kg doxorubicin on days 5 and 10. Investigator was not blinded to treatment group.

EL4 Subcutaneous Tumor Models. 6–8 week old female C57BL/6 mice were used (Charles River). Five million EL4 cells were prepared in HBSS and injected subcutaneously on the right flank of sedated (ketamine/xylazine) mice (day 0) in a 100 μL volume. Mice were randomized into four treatment groups: vehicle, PAC-1 alone, doxorubicin alone, and PAC-1 + dox. PAC-1 was formulated in HPβCD (13.3 mg/mL in 200 mg/mL HPβCD at pH 5.5). Doxorubicin was formulated in 0.9% saline (0.5 mg/mL). Mice were treated one or three times daily on days 1–9 with 100 mg/kg PAC-1 as an IP injection. Mice were treated with doxorubicin on days 3 and 7 with 7.5 mg/kg doxorubicin as an IP injection. All mice within a model received an equal number of treatments, with HPβCD or saline vehicles substituted for mice not receiving active drug. After 10 days, the largest tumors had achieved maximal size, >1500 mm³; mice were sacrificed, and tumors were excised and weighed.

Evaluation of Doxorubicin-Induced Toxicity in BALB/c Mice. BALB/c mice (6–8 week old female, Charles River) were treated as described in the chronic dosing model (mice were treated daily from days 1–15 with 125 mg/kg PAC-1 orally, and with 7.5 mg/kg doxorubicin on days 5 and 10). All animals were sacrificed on day 16. The hearts excised and fixed in 10% neutral-buffered formalin, embedded in paraffin and stained with hematoxylin-eosin. Alterations were evaluated semiquantitatively by light microscopy analysis of sections and scored from 0 to 3,⁶⁶ based on the percentage of myocytes displaying myofibrillar loss and cytoplasmic vacuolization: 0, no alteration; 1, <5%; 1.5, 5%–15%; 2.0, 16%–25%; 2.5, 26%–35%; and 3, >35% of the myocardial cells showing damage. Investigator was blinded to treatment group. Representative images from each treatment group were obtained.

Anticancer Assessment of PAC-1 and Doxorubicin in Dogs with Lymphoma or Osteosarcoma. Inclusion

Criteria. The inclusion criteria for eligible patients were the following: histologically or cytologically confirmed multicentric lymphoma or osteosarcoma, measurable tumor burden, favorable performance status, a life expectancy of >4 weeks, and no significant comorbid illness including renal or hepatic failure, history of congestive heart failure, or clinical coagulopathy. Pet owners signed a written informed consent form prior to study entry according to university guidelines.

Canine patients receiving biweekly dosing of bolus high dose PAC-1 received 75–100 mg/kg of PAC-1 (oral), which was followed by 20–30 mg/m² doxorubicin (IV) 4 h later. Canine patients receiving daily dosing of PAC-1 received between 10 and 13 mg/kg of PAC-1 (oral) daily, and 25 mg/m² doxorubicin (IV) every 14 days.

Tumor size was monitored via digital radiography scans and caliper measurement when possible. Measurement was performed according to the Response Evaluation Criteria in Solid Tumors (RECIST) method. Briefly, the longest linear length measurement was recorded for each tumor, with the summation of these values giving a RECIST score.

Statistical Analysis. For cell culture assays, all values reported are the average of ≥3 biologic replicates. Data are represented as the mean and error bars represent the standard error across biologic replicates. Comparison of survival curves was performed using GraphPad Prism and the Gehan-Breslow-Wilcoxon method was used to compare curves. For subcutaneous tumor models, paired sample, two-tailed, *t* tests were used to determine significant differences in tumor burden between treatment groups. All data were normally distributed and the variances were similar between the groups being statistically compared. Sample size was based on previous experience with experimental variability, and no statistical method was used to predetermine sample sizes. No samples were excluded from the analysis. A *P* value of <0.05 was considered significant.

■ ASSOCIATED CONTENT

● Supporting Information

The Supporting Information is available free of charge on the ACS Publications website at DOI: [10.1021/acscentsci.6b00165](https://doi.org/10.1021/acscentsci.6b00165).

Supporting Figures S1–S11 and Table S1 (PDF)

■ AUTHOR INFORMATION

Corresponding Author

*E-mail: hergenro@illinois.edu.

Notes

The authors declare the following competing financial interest(s): The University of Illinois has filed patents on compounds in this manuscript.

■ ACKNOWLEDGMENTS

We are grateful to the National Institutes of Health (Grant R01-CA120439), The V Foundation for Cancer Research, and the University of Illinois for support of this work. R.C.B. is a National Science Foundation predoctoral fellow, a Robert C. and Carolyn J. Springborn graduate fellow, and a member of the NIH Chemistry-Biology Interface Training Program (Grant NRSA 1-T32-GM070421). H.S.R. was partially supported by the Richard B. Silverman Predoctoral Fellowship from the American Chemical Society Division of Medicinal Chemistry.

■ DEDICATION

This manuscript is dedicated to Professor Stuart L. Schreiber on the occasion of his 60th birthday.

■ REFERENCES

- (1) Schmitt, M. W.; Loeb, L. A.; Salk, J. J. The influence of subclonal resistance mutations on targeted cancer therapy. *Nat. Rev. Clin. Oncol.* **2015**, *13*, 335–347.
- (2) DeVita, V. T., Jr.; Chu, E. A history of cancer chemotherapy. *Cancer Res.* **2008**, *68*, 8643–8653.
- (3) Doroshow, J. H.; Kummur, S. Translational research in oncology—10 years of progress and future prospects. *Nat. Rev. Clin. Oncol.* **2014**, *11*, 649–662.
- (4) Huang, M.; Shen, A.; Ding, J.; Geng, M. Molecularly targeted cancer therapy: some lessons from the past decade. *Trends Pharmacol. Sci.* **2014**, *35*, 41–50.
- (5) Engelman, J. A.; Settleman, J. Acquired resistance to tyrosine kinase inhibitors during cancer therapy. *Curr. Opin. Genet. Dev.* **2008**, *18*, 73–79.
- (6) O'Hare, T.; Zabriske, M. S.; Eiring, A. M.; Deininger, M. W. Pushing the limits of targeted therapy in chronic myeloid leukaemia. *Nat. Rev. Cancer* **2012**, *12*, 513–526.
- (7) Groenendijk, F. H.; Bernards, R. Drug resistance to targeted therapies: déjà vu all over again. *Mol. Oncol.* **2014**, *8*, 1067–1083.
- (8) Slamon, D. J.; Leyland-Jones, B.; Shak, S.; Fuchs, H.; Paton, V.; Bajamonde, A.; Fleming, T.; Eiermann, W.; Wolter, J.; Pegram, M.; et al. Use of chemotherapy plus a monoclonal antibody against HER2 for metastatic breast cancer that overexpresses HER2. *N. Engl. J. Med.* **2001**, *344*, 783–792.
- (9) Coiffier, B.; Lepage, E.; Briere, J.; Herbrecht, R.; Tilly, H.; Bouabdallah, R.; Morel, P.; Van den Neste, E.; Salles, G.; Gaulard, P.; et al. CHOP chemotherapy plus rituximab compared with CHOP alone in elderly patients with diffuse large-B-cell lymphoma. *N. Engl. J. Med.* **2002**, *346*, 235–242.
- (10) Sandler, A.; Gray, R.; Perry, M. C.; Brahmer, J.; Schiller, J. H.; Dowlati, A.; Lilienbaum, R.; Johnson, D. H. Paclitaxel-carboplatin alone or with bevacizumab for non-small-cell lung cancer. *N. Engl. J. Med.* **2006**, *355*, 2542–2550.
- (11) Jain, R. K.; Duda, D. G.; Clark, J. W.; Loeffler, J. S. Lessons from phase III clinical trials on anti-VEGF therapy for cancer. *Nat. Clin. Pract. Oncol.* **2006**, *3*, 24–40.
- (12) Green, M. R. Targeting Targeted Therapy. *N. Engl. J. Med.* **2004**, *350*, 2191–2193.
- (13) Bielack, S. S.; Smeland, S.; Whelan, J. S.; Marina, N.; Jovic, G.; Hook, J. M.; Krailo, M. D.; Gebhardt, M.; Papai, Z.; Meyer, J.; et al. Methotrexate, Doxorubicin, and Cisplatin (MAP) Plus Maintenance Pegylated Interferon Alfa-2b Versus MAP Alone in Patients With Resectable High-Grade Osteosarcoma and Good Histologic Response to Preoperative MAP: First Results of the EURAMOS-1 Good Response Randomized Controlled Trial. *J. Clin. Oncol.* **2015**, *33*, 2279–2287.
- (14) World Health Organization.; Stop TB Initiative (World Health Organization) *Treatment of Tuberculosis: Guidelines*; 4th ed.; World Health Organization: Geneva, 2010.
- (15) Soini, Y.; Paakko, P. Apoptosis and expression of caspases 3, 6 and 8 in malignant non-Hodgkin's lymphomas. *A P M I S* **1999**, *107*, 1043–1050.
- (16) Chen, N.; Gong, J.; Chen, X.; Meng, W.; Huang, Y.; Zhao, F.; Wang, L.; Zhou, Q. Caspases and inhibitor of apoptosis proteins in cutaneous and mucosal melanoma: expression profile and clinicopathologic significance. *Hum. Pathol.* **2009**, *40*, 950–956.
- (17) Krepela, E.; Prochazka, J.; Liu, X.; Fiala, P.; Kinkor, Z. Increased expression of Apaf-1 and procaspase-3 and the functionality of intrinsic apoptosis apparatus in non-small cell lung carcinoma. *Biol. Chem.* **2004**, *385*, 153–168.
- (18) Nakopoulou, L.; Alexandrou, P.; Stefanaki, K.; Panayotopoulou, E.; Lazaris, A. C.; Davaris, P. S. Immunohistochemical expression of caspase-3 as an adverse indicator of the clinical outcome in human breast cancer. *Pathobiology* **2002**, *69*, 266–273.
- (19) Roth, H. S.; Hergenrother, P. J. Derivatives of Procaspase-Activating Compound 1 (PAC-1) and their Anticancer Activities. *Curr. Med. Chem.* **2016**, *23*, 201–241.
- (20) Crawford, E. D.; Wells, J. A. Caspase substrates and cellular remodeling. *Annu. Rev. Biochem.* **2011**, *80*, 1055–1087.
- (21) Zorn, J. A.; Wolan, D. W.; Agard, N. J.; Wells, J. A. Fibrils colocalize caspase-3 with procaspase-3 to foster maturation. *J. Biol. Chem.* **2012**, *287*, 33781–33795.
- (22) Bose, K.; Pop, C.; Feeney, B.; Clark, A. C. An uncleavable procaspase-3 mutant has a lower catalytic efficiency but an active site similar to that of mature caspase-3. *Biochemistry* **2003**, *42*, 12298–12310.
- (23) Shin, S.; Sung, B. J.; Cho, Y. S.; Kim, H. J.; Ha, N. C.; Hwang, J. I.; Chung, C. W.; Jung, Y. K.; Oh, B. H. An anti-apoptotic protein human survivin is a direct inhibitor of caspase-3 and -7. *Biochemistry* **2001**, *40*, 1117–1123.
- (24) Deveraux, Q. L.; Takahashi, R.; Salvesen, G. S.; Reed, J. C. X-linked IAP is a direct inhibitor of cell-death proteases. *Nature* **1997**, *388*, 300–304.
- (25) Perry, D. K.; Smyth, M. J.; Stennicke, H. R.; Salvesen, G. S.; Duriez, P.; Poirier, G. G.; Hannun, Y. A. Zinc is a potent inhibitor of the apoptotic protease, caspase-3. A novel target for zinc in the inhibition of apoptosis. *J. Biol. Chem.* **1997**, *272*, 18530–18533.
- (26) Truong-Tran, A. Q.; Grosser, D.; Ruffin, R. E.; Murgia, C.; Zalewski, P. D. Apoptosis in the normal and inflamed airway epithelium: role of zinc in epithelial protection and procaspase-3 regulation. *Biochem. Pharmacol.* **2003**, *66*, 1459–1468.
- (27) Carter, J. E.; Truong-Tran, A. Q.; Grosser, D.; Ho, L.; Ruffin, R. E.; Zalewski, P. D. Involvement of redox events in caspase activation in zinc-depleted airway epithelial cells. *Biochem. Biophys. Res. Commun.* **2002**, *297*, 1062–1070.
- (28) Peterson, Q. P.; Goode, D. R.; West, D. C.; Ramsey, K. N.; Lee, J. J.; Hergenrother, P. J. PAC-1 activates procaspase-3 in vitro through relief of zinc-mediated inhibition. *J. Mol. Biol.* **2009**, *388*, 144–158.
- (29) Stennicke, H. R.; Salvesen, G. S. Biochemical characteristics of caspases-3, -6, -7, and -8. *J. Biol. Chem.* **1997**, *272*, 25719–25723.
- (30) Daniel, A. G.; Peterson, E. J.; Farrell, N. P. The bioinorganic chemistry of apoptosis: potential inhibitory zinc binding sites in caspase-3. *Angew. Chem., Int. Ed.* **2014**, *53*, 4098–4101.
- (31) West, D. C.; Qin, Y.; Peterson, Q. P.; Thomas, D. L.; Palchadhuri, R.; Morrison, K. C.; Lucas, P. W.; Palmer, A. E.; Fan, T. M.; Hergenrother, P. J. Differential effects of procaspase-3 activating compounds in the induction of cancer cell death. *Mol. Pharmaceutics* **2012**, *9*, 1425–1434.
- (32) Wang, F.; Wang, L.; Zhao, Y.; Li, Y.; Ping, G.; Xiao, S.; Chen, K.; Zhu, W.; Gong, P.; Yang, J.; et al. A novel small-molecule activator of procaspase-3 induces apoptosis in cancer cells and reduces tumor growth in human breast, liver and gallbladder cancer xenografts. *Mol. Oncol.* **2014**, *8*, 1640–1652.
- (33) Putt, K. S.; Chen, G. W.; Pearson, J. M.; Sandhorst, J. S.; Hoagland, M. S.; Kwon, J. T.; Hwang, S. K.; Jin, H.; Churchwell, M. I.; Cho, M. H.; et al. Small-molecule activation of procaspase-3 to caspase-3 as a personalized anticancer strategy. *Nat. Chem. Biol.* **2006**, *2*, 543–550.
- (34) Putinski, C.; Abdul-Ghani, M.; Stiles, R.; Brunette, S.; Dick, S. A.; Fernando, P.; Megeney, L. A. Intrinsic-mediated caspase activation is essential for cardiomyocyte hypertrophy. *Proc. Natl. Acad. Sci. U. S. A.* **2013**, *110*, E4079–4087.
- (35) Peterson, Q. P.; Hsu, D. C.; Novotny, C. J.; West, D. C.; Kim, D.; Schmit, J. M.; Dirikolu, L.; Hergenrother, P. J.; Fan, T. M. Discovery and canine preclinical assessment of a nontoxic procaspase-3-activating compound. *Cancer Res.* **2010**, *70*, 7232–7241.
- (36) Botham, R. C.; Fan, T. M.; Im, I.; Borst, L. B.; Dirikolu, L.; Hergenrother, P. J. Dual small-molecule targeting of procaspase-3 dramatically enhances zymogen activation and anticancer activity. *J. Am. Chem. Soc.* **2014**, *136*, 1312–1319.

- (37) Patel, V.; Balakrishnan, K.; Keating, M. J.; Wierda, W. G.; Gandhi, V. Expression of executioner procaspases and their activation by a procaspase-activating compound in chronic lymphocytic leukemia cells. *Blood* **2015**, *125*, 1126–1136.
- (38) Peh, J.; Fan, T. M.; Wycislo, K. L.; Roth, H. S.; Hergenrother, P. J. The combination of vemurafenib and procaspase-3 activation is synergistic in mutant BRAF melanomas. *Mol. Cancer Ther.* **2016**, DOI:10.1158/1535-7163.MCT-16-0025.
- (39) Razi, S. S.; Rehmani, S.; Li, X. G.; Park, K.; Schwartz, G. S.; Latif, M. J.; Bhora, F. Y. Antitumor activity of paclitaxel is significantly enhanced by a novel proapoptotic agent in non-small cell lung cancer. *J. Surg. Res.* **2015**, *194*, 622–630.
- (40) Huang, J. Q.; Liang, H. L.; Zhang, X. C.; Xie, Z.; Jin, T. E. Synergistic antitumor activity of pro-apoptotic agent PAC-1 with cisplatin by the activation of CASP3 in pulmonary adenocarcinoma cell line H1299. *Asia Pac J. Clin Oncol* **2016**, *12*, 41–51.
- (41) Lucas, P. W.; Schmit, J. M.; Peterson, Q. P.; West, D. C.; Hsu, D. C.; Novotny, C. J.; Dirikolu, L.; Churchwell, M. I.; Doerge, D. R.; Garrett, L. D.; et al. Pharmacokinetics and derivation of an anticancer dosing regimen for PAC-1, a preferential small molecule activator of procaspase-3, in healthy dogs. *Invest. New Drugs* **2011**, *29*, 901–911.
- (42) Chou, T. C.; Talalay, P. Quantitative-Analysis of Dose-Effect Relationships - the Combined Effects of Multiple-Drugs or Enzyme-Inhibitors. *Adv. Enzyme Regul.* **1984**, *22*, 27–55.
- (43) Weiss, R. B. The anthracyclines: will we ever find a better doxorubicin? *Semin. Oncol.* **1992**, *19*, 670–686.
- (44) Minotti, G.; Menna, P.; Salvatorelli, E.; Cairo, G.; Gianni, L. Anthracyclines: molecular advances and pharmacologic developments in antitumor activity and cardiotoxicity. *Pharmacol. Rev.* **2004**, *56*, 185–229.
- (45) Tewey, K. M.; Rowe, T. C.; Yang, L.; Halligan, B. D.; Liu, L. F. Adriamycin-induced DNA damage mediated by mammalian DNA topoisomerase II. *Science* **1984**, *226*, 466–468.
- (46) Zhang, S.; Liu, X.; Bawa-Khalife, T.; Lu, L. S.; Lyu, Y. L.; Liu, L. F.; Yeh, E. T. Identification of the molecular basis of doxorubicin-induced cardiotoxicity. *Nat. Med.* **2012**, *18*, 1639–1642.
- (47) Ewer, M. S.; Ewer, S. M. Cardiotoxicity of anticancer treatments. *Nat. Rev. Cardiol.* **2015**, *12*, 547–558.
- (48) BurrIDGE, P. W.; Li, Y. F.; Matsa, E.; Wu, H.; Ong, S. G.; Sharma, A.; Holmstrom, A.; Chang, A. C.; Coronado, M. J.; Ebert, A. D.; et al. Human induced pluripotent stem cell-derived cardiomyocytes recapitulate the predilection of breast cancer patients to doxorubicin-induced cardiotoxicity. *Nat. Med.* **2016**, *22*, 547–556.
- (49) Tomasz, M. Mitomycin C: small, fast and deadly (but very selective). *Chem. Biol.* **1995**, *2*, 575–579.
- (50) Bradner, W. T. Mitomycin C: a clinical update. *Cancer Treat. Rev.* **2001**, *27*, 35–50.
- (51) Khanna, C.; Prehn, J.; Yeung, C.; Caylor, J.; Tsokos, M.; Helman, L. An orthotopic model of murine osteosarcoma with clonally related variants differing in pulmonary metastatic potential. *Clin. Exp. Metastasis* **2000**, *18*, 261–271.
- (52) Roth, H. S.; Botham, R. C.; Schmid, S. C.; Fan, T. M.; Dirikolu, L.; Hergenrother, P. J. Removal of metabolic liabilities enables development of derivatives of procaspase-activating compound 1 (PAC-1) with improved pharmacokinetics. *J. Med. Chem.* **2015**, *58*, 4046–4065.
- (53) Gould, S. E.; Junttila, M. R.; de Sauvage, F. J. Translational value of mouse models in oncology drug development. *Nat. Med.* **2015**, *21*, 431–439.
- (54) Schiffman, J. D.; Breen, M. Comparative oncology: what dogs and other species can teach us about humans with cancer. *Philos. Trans. R. Soc., B* **2015**, *370*. DOI:10.1098/rstb.2014.0231
- (55) Ranieri, G.; Gadaleta, C. D.; Patruno, R.; Zizzo, N.; Daidone, M. G.; Hansson, M. G.; Paradiso, A.; Ribatti, D. A model of study for human cancer: Spontaneous occurring tumors in dogs. Biological features and translation for new anticancer therapies. *Crit. Rev. Oncol Hematol* **2013**, *88*, 187–197.
- (56) Paoloni, M.; Khanna, C. Translation of new cancer treatments from pet dogs to humans. *Nat. Rev. Cancer* **2008**, *8*, 147–156.
- (57) Paoloni, M.; Davis, S.; Lana, S.; Withrow, S.; Sangiorgi, L.; Picci, P.; Hewitt, S.; Triche, T.; Meltzer, P.; Khanna, C. Canine tumor cross-species genomics uncovers targets linked to osteosarcoma progression. *BMC Genomics* **2009**, *10*, 625.
- (58) Mueller, F.; Fuchs, B.; Kaser-Hotz, B. Comparative biology of human and canine osteosarcoma. *Anticancer Res.* **2007**, *27*, 155–164.
- (59) Szewczyk, M.; Lechowski, R.; Zabielska, K. What do we know about canine osteosarcoma treatment? Review. *Vet. Res. Commun.* **2015**, *39*, 61–67.
- (60) Marconato, L.; Gelain, M. E.; Comazzi, S. The dog as a possible animal model for human non-Hodgkin lymphoma: a review. *Hematol. Oncol.* **2013**, *31*, 1–9.
- (61) Breen, M.; Modiano, J. F. Evolutionarily conserved cytogenetic changes in hematological malignancies of dogs and humans—man and his best friend share more than companionship. *Chromosome Res.* **2008**, *16*, 145–154.
- (62) Ogilvie, G. K.; Straw, R. C.; Jameson, V. J.; Walters, L. M.; Lafferty, M. H.; Powers, B. E.; Withrow, S. J. Evaluation of single-agent chemotherapy for treatment of clinically evident osteosarcoma metastases in dogs: 45 cases (1987–1991). *J. Am. Vet. Med. Assoc.* **1993**, *202*, 304–306.
- (63) Keller, E. T.; MacEwen, E. G.; Rosenthal, R. C.; Helfand, S. C.; Fox, L. E. Evaluation of prognostic factors and sequential combination chemotherapy with doxorubicin for canine lymphoma. *J. Vet. Intern. Med.* **1993**, *7*, 289–295.
- (64) Baskin, C. R.; Couto, C. G.; Wittum, T. E. Factors influencing first remission and survival in 145 dogs with lymphoma: a retrospective study. *J. Am. Anim. Hosp. Assoc.* **2000**, *36*, 404–409.
- (65) Yalcin, E.; Oruc, E.; Cavusoglu, K.; Yapar, K. Protective role of grape seed extract against doxorubicin-induced cardiotoxicity and genotoxicity in albino mice. *J. Med. Food* **2010**, *13*, 917–925.
- (66) Herman, E. H.; Zhang, J.; Ferrans, V. J. Comparison of the protective effects of desferrioxamine and ICRF-187 against doxorubicin-induced toxicity in spontaneously hypertensive rats. *Cancer Chemother. Pharmacol.* **1994**, *35*, 93–100.
- (67) Jaffe, N. Historical perspective on the introduction and use of chemotherapy for the treatment of osteosarcoma. *Adv. Exp. Med. Biol.* **2014**, *804*, 1–30.
- (68) Smith, M. A.; Ungerleider, R. S.; Horowitz, M. E.; Simon, R. Influence of doxorubicin dose intensity on response and outcome for patients with osteogenic sarcoma and Ewing's sarcoma. *J. Natl. Cancer Inst* **1991**, *83*, 1460–1470.
- (69) Link, M. P.; Goorin, A. M.; Miser, A. W.; Green, A. A.; Pratt, C. B.; Belasco, J. B.; Pritchard, J.; Malpas, J. S.; Baker, A. R.; Kirkpatrick, J. A.; et al. The effect of adjuvant chemotherapy on relapse-free survival in patients with osteosarcoma of the extremity. *N. Engl. J. Med.* **1986**, *314*, 1600–1606.
- (70) Dernell, W. S.; Ehrhart, N. P.; Straw, R. C.; Vail, D. M. In *Withrow & MacEwen's Small Animal Clinical Oncology*, 4th ed.; W.B. Saunders: St. Louis, 2007.
- (71) Singh, K. K.; Shukla, P. C.; Quan, A.; Desjardins, J. F.; Lovren, F.; Pan, Y.; Garg, V.; Gosal, S.; Garg, A.; Szmítko, P. E.; et al. BRCA2 protein deficiency exaggerates doxorubicin-induced cardiomyocyte apoptosis and cardiac failure. *J. Biol. Chem.* **2012**, *287*, 6604–6614.
- (72) Gianni, L.; Salvatorelli, E.; Minotti, G. Anthracycline cardiotoxicity in breast cancer patients: synergism with trastuzumab and taxanes. *Cardiovasc. Toxicol.* **2007**, *7*, 67–71.
- (73) BurrIDGE, P. W.; Li, Y. F.; Matsa, E.; Wu, H.; Ong, S.-G.; Sharma, A.; Holmstrom, A.; Chang, A. C.; Coronado, M. J.; Ebert, A. D.; et al. Human induced pluripotent stem cell-derived cardiomyocytes recapitulate the predilection of breast cancer patients to doxorubicin-induced cardiotoxicity. *Nat. Med.* **2016**, *22*, 547–556.
- (74) Palchaudhuri, R.; Lambrecht, M. J.; Botham, R. C.; Partlow, K. C.; van Ham, T. J.; Putt, K. S.; Nguyen, L. T.; Kim, S. H.; Peterson, R. T.; Fan, T. M.; et al. A small molecule that induces intrinsic pathway apoptosis with unparalleled speed. *Cell Rep.* **2015**, *13*, 2027–2036.